Chapter 14

Laboratory Measurements of Velocity and Attenuation in Sediments

M. Prasad[1], *M. A. Zimmer*[1], *P. A. Berge*[2], *and B. P. Bonner*[2]

Introduction

Seismic velocities and attenuations collected in the field with, for example, reflection, refraction, and cross-hole surveys serve as valuable constraints on subsurface lithology, porosity, permeability, and fluid saturation. Until recently, the measurement resolution of seismic velocities in the shallow subsurface had limited the use of the complete power of seismic attribute analysis in shallow soils. Recent advances in field techniques for seismic measurements in shallow soils (e.g., Bachrach et al., 1998; Bachrach and Mukerji, this volume; Baker et al., 1999; Carr et al., 1998; Steeples et al., 1999) as well as the development of seismic cone penetration tests (SCPT) and other improved geotechnical methods (e.g., Crouse et al., 1993; Boulanger et al., 1998) have begun to permit the application of seismic attribute analysis to shallow soils. Unfortunately, the laboratory studies required for establishing relations between the physical properties of the soils and their seismic properties have not been extended to the low pressures analogous to these shallow depths, so the effects of lithology, fluid saturation, and compaction on seismic (P- and S-wave) properties of shallow soils are largely unknown.

Interpretation of shallow seismic data requires knowledge about P-wave and, to a lesser extent, S-wave propagation in sediments at low pressures. A wealth of geotechnical literature exists in measurements of shear modulus at low pressures (e.g., Santamarina et al., 2001). Often, these measurements lack P-wave information, which is crucial for field seismic studies. In geophysical literature, the focus has been mainly for oil industry application. Thus, the effects of physical properties and fluid content on the seismic properties of sedimentary rocks have been studied extensively at higher pressures using ultrasonic measurements and other laboratory techniques (e.g., Domenico, 1976; Cheng, 1978; Han et al., 1986; Wilkens et al., 1986; Knight and Nolen-Hoeksema, 1990; Vernik and Nur, 1992; Green et al., 1993; Prasad and Manghnani, 1997). Interpretation methods in common use for seismic field data have been developed for oil industry applications (e.g., Wyllie et al., 1956; Kuster and Toksöz, 1974). They are not optimized for the shallow depths and unconsolidated materials of environmental or engineering applications. P- and S-wave laboratory data collected for soils at low-pressure conditions appropriate to the near surface are sparse in the literature. Although laboratory data sets are available in the exploration geophysics, marine geophysics, and soil mechanics literature (e.g., Rao, 1966; Domaschuk and Wade, 1969; Domenico, 1976; Hamilton and Bachman, 1982; Prasad and Meissner, 1992; Santamarina et al., 2001), few studies (Hamilton and Bachman, 1982; Zimmer et al., 2000; 2002a; Prasad, 2002) include both compressional and shear-wave velocity measurements as a function of pressure at the extremely low pressures representing the shallow subsurface. Relevant laboratory measurements of soil properties will enable us to develop new interpretation techniques for seismic field data for environmental and engineering applications.

To this end, we describe state-of-the-art laboratory experiments involving the measurement of ultrasonic velocities at low pressures in unconsolidated sediments and summarize the main velocity results. The ongoing experiments at Stanford University and Lawrence Livermore National Laboratory (LLNL) were developed to make accurate measurements of compressional-wave (V_P, Q_p) and shear-wave (V_S, Q_S) velocities and attenuations in highly attenuating soils at low pressures (e.g., Aracne-Ruddle et al., 1998, 1999; Bonner et al., 1999a, 2000, 2001; Zimmer et al., 2002a, Zimmer et al., 2002b; Prasad, 2002). The data presented here include LLNL uniaxial measurements on dry, saturated, and partially saturated sands and sand-clay mixtures made at pressures below approximately 0.1 MPa; and Stanford hydrostatic measurements made on dry and water-saturated sands at pressures from 0.1 MPa to 20 MPa. Also presented here are velocity-pressure transforms developed from the Stanford data for predicting V_P and V_S. Methods developed from the LLNL data for relating velocities to lithology are described elsewhere (for example, Bertete-Aguirre and Berge, 2002). The LLNL and Stanford ultrasonic velocity measurements for unconsolidated soils at low stresses confirm recent field observations of extremely low seismic velocities in shallow soils (e.g., Bachrach et al., 1998; Carr et al., 1998; Steeples et al., 1999). These experimental results should allow for the development of empirical and theoretical models that will

[1]Geophysics Department, Stanford University, Stanford, CA 94305. E-mail: manika.prasad@stanford.edu, zimmer@pangea.stanford.edu.

[2]Experimental Geophysics Group, Lawrence Livermore National Laboratory, 7000 East Ave., Livermore, CA 94550. E-mail: bonner1@llnl.gov, berge1@llnl.gov.

permit more accurate inversions of shallow seismic data for the physical properties and fluid content of soft soils (e.g., Bertete-Aguirre and Berge, 2002; Berge and Bonner, 2002). Such seismic interpretation methods can help guide effective in-situ environmental remediation and foundation engineering.

Experimental Methods

Laboratory experiments under well-controlled conditions allow us to understand the physics of wave propagation in sediments and to develop predictive empirical relations. It has been standard geophysical laboratory practice to conduct such experiments on rocks typically at 1-MHz frequency under high confining pressures. Considerable design efforts are required to modify such experiments to overcome experimental challenges and simulate shallow soil conditions in the laboratory. For example,

1) Very low pressures must be maintained in experiments to simulate the in-situ conditions of shallow soils.
2) Experimental design should avoid impedance mismatch between standard high-impedance acoustic transmitters and low-impedance soils. Thus, the commonly used high-impedance metal transducer plates need to be replaced with plates made from low impedance materials.
3) High signal amplitude and high signal-to-noise ratio must be maintained: Since unconsolidated sediments are highly attenuating, high signal energy is necessary to propagate elastic waves through them. Using lower frequencies reduces attenuation and produces a higher energy signal.

We report here two different types of equipment to simulate very low pressures and generate a high signal output to propagate through unconsolidated materials. One experiment (called the LLNL experiment) was designed to measure ultrasonic velocities in sediments at dry, fully and partially saturated conditions under uniaxial loads up to 0.1 MPa. The second experiment (called the Stanford experiment) was designed to measure velocities in sediments at dry and at fully saturated conditions under confining pressures up to 20 MPa. Special care was taken to ensure generation of interpretable signals at low pressures of 0.1 MPa.

The LLNL experimental setup

In the Experimental Geophysics Laboratory at LLNL, we used the pulse transmission technique (Sears and Bonner, 1981) to measure ultrasonic compressional and shear-wave velocities for dry and fully saturated sediments. We also measured velocities in sand samples with various degrees of partial saturation (Bonner et al., 2001).

Measurements were made on 4.49-cm-long cylinders with 4.7-cm diameter at room temperature and at pressures between about 0.01 and about 0.1 MPa to simulate the top few meters of the subsurface. In order to obtain good ultrasonic signals at these low pressures, the transmitting transducer was driven with unusually high voltages, approaching the dielectric breakdown. The transducers were also operated at frequencies at the low end of the available range, from about 100 to 500 kHz. A low noise, high-gain preamplifier was needed and extensive signal averaging was used to improve the signal-to-noise ratio. High-insertion-loss sample containers were required to suppress arrivals that travel around the sample to obscure true arrivals, to make it possible to detect shear waves in unconsolidated samples at low pressures. The sample containers provided over 100 dB insertion loss to control leakage of ultrasound, by using geometric constraints to suppress low frequencies and material selection to attenuate high frequencies (Bonner et al., 1999b). The sample assemblies were closed with latex membranes that transmitted sound from the transducer and contained the soil mixture. Precision (repeatability of measurements) was limited to 20% at the lowest stresses near 1 psi (0.007 MPa), but improved with signal amplitude to about 3% for compressional (P) waves and 10% for shear (S) waves at higher stresses. Accuracy in timing the arrivals (uncertainity of first arrival picks) was about 1% for P and 2% to 5% for S arrivals in most cases. Sample length change was less than 0.1% at the highest pressures and thus was considered negligible. Details of the experimental procedures are given in Aracne-Ruddle et al. (1999).

Up to several meters of overburden were simulated by applying low uniaxial stress up to about 0.1 MPa to the sample using a pneumatic system. Although the sample sleeve was not perfectly rigid, the internal stress in the sample approximately corresponded to the uniaxial strain condition. Pore fluid pressures, applied using a regulated gas tank (Figure 1), could be increased beyond the sample bubble pressure to expel water and produce partial saturation. Tensiometers were used to measure the pressure in the continuous aqueous phase when the sample was partially saturated. The difference between applied and water-phase pressure is the capillary pressure. Results of LLNL measurements for some samples are presented later in this chapter.

The Stanford experimental setup

The apparatus developed in the Rock Physics Laboratory at Stanford University used pulse transmission to measure the ultrasonic P- and S-wave velocities and attenuations of unconsolidated sands at hydrostatic pressures from 100 kPa to 20 MPa. Zimmer et al. (2000; 2002a) have described details of the experimental setup; the main features are given here. The apparatus consists of a sample

holder (Figure 2a) that is placed into a pressure vessel (Figure 2b) capable of producing confining pressures of up to 20 MPa. The samples are 3.8 cm in diameter and about 3 cm in length. The sample holder consists of two end caps that contain the ultrasonic transducers and that are supported in a steel frame. The transducers were constructed with lower (200 kHz) than traditional ultrasonic (1 MHz) frequency piezoelectric crystals and with low-impedance face plates made out of a glass-filled polycarbonate to maximize the elastic wave-energy propagated through the sample. The sample holder was also designed to be disassembled and reassembled easily, and can be placed in the pressure vessel with minimal disturbance. These features were necessary in order to permit consistent sample preparation so as not to obscure the effects of the textural variations of the sands on the ultrasonic measurements. With this arrangement we were able to get interpretable shear-wave signals through saturated samples at pressures as low as 100 kPa. An error analysis that took into account errors in the length measurements, the measurement of the delay times, and ambiguities in the pick of arrival times gave error estimates of about 2% for the V_P values, and about 4% for the V_S values over the entire pressure range (Zimmer et al., 2002a).

The static strain on the sample was registered using three axial gauges that measured the length change between the end caps and one circumferential gauge that measured the change in the circumference of the middle of the sample. The axial measurements allowed us to determine accurately the length of the sample and to detect any tilting of the end caps relative to each other. The circumferential gauge allowed us to make better estimates of the volume and porosity of the sample, as it told us how much the sample deviated from a purely cylindrical shape.

The next section of this chapter describes some of the LLNL and Stanford samples, and following sections summarize and discuss some measurement results.

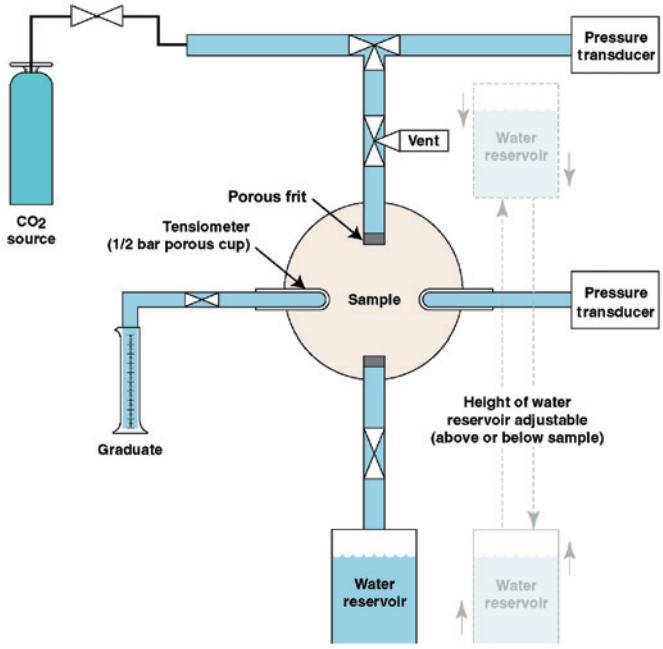

Figure 1. Schematic diagram of pore fluid pumping system for LLNL apparatus.

a) b)

Figure 2. (a) The Stanford sample holder. (b) The Stanford pressure vessel in its stand.

Samples

The sediments used in both the LLNL and the Stanford experiments were made artificially in order to study the relations between sediment texture (that is, porosity, composition, and compaction) and its seismic properties under well-defined and reproducible conditions. In the LLNL experiments, sand and sand-clay mixtures were measured. The Stanford experiments were made on natural sands. Both experiments were first made to understand the physical processes in sediments. Future research will concentrate on effects of fabric differences between artificial samples and natural soils.

LLNL sand-clay and sand samples

The artificial sediment samples that LLNL made were fabricated from Ottawa sand mixed with a swelling clay. The sand comes from a quarry near the city of Ottawa, Illinois and is Middle Ordovician in age. It is composed entirely of well-rounded quartz grains (Domenico, 1976). The sand was sieved to a median grain diameter of 273 μm, with grain sizes ranging from 74 to 420 μm. The clay was Wyoming bentonite, a sodium montmorillonite from Wyoming that is a swelling smectite. The clay was equilibrated in a 100% humid atmosphere for seven days before sample preparation, in order to achieve reproducible water content. The clay content in the sand-clay samples was 1 to 40% by mass. Bulk density ranged from about 1400 to 1700 kg/m^3, where the lowest density corresponded to the sample having 40% clay by mass and pure sand samples had densities of about 1700 kg/m^3. We found that the packing affected measured velocities and their load dependence. We were able to achieve reproducible results using a hand-held brass weight that fit snugly in the sample holder. Sample preparation and composition are discussed in detail in Aracne-Ruddle et al. (1999) and Bonner et al. (2001).

Stanford sand samples for hydrostatic experiments

The measurements collected with the hydrostatic apparatus at Stanford were all made on samples of the Santa Cruz aggregate, a fine-grained, well-sorted, angular quartz sand from Santa Cruz, California. We prepared water-saturated samples first sliding the jacket over the lower end cap and then filling it with water. The sand was then poured slowly into the water and was stirred slightly to allow any air bubbles to escape and to level off the top of the sample. The upper end cap was then slid into the jacket above the sample until it just rested on the top of the sand, so the sand was not precompacted. The sample holder was then assembled and placed into the pressure vessel. To ensure repeatability and yet maintain high initial porosity, dry samples were prepared by air pluviating the sand into the jacket, and then leveling off the top by placing a 160 g aluminum weight on top of the sand about 20 times.

Once the sample holder was placed in the pressure vessel, measurements were made at regular pressure steps as the pressure was cycled through one to five pressure cycles, with each cycle peaking at a slightly higher pressure up to 20 MPa. The measurement results from two water-saturated sand samples and two dry sand samples are presented in the results section of this paper. Typical waveforms for P- and S-waves in a sand sample at two pressures (0.05 and 20 MPa) are shown in Figure 3a-d.

Results

V_P and V_S results for sands and sand-clay mixtures from the LLNL experiments

Figure 4a and b presents LLNL results for V_P and V_S with respect to pressure for dry sands and sand-clay mixtures. The pressures are equivalent to about the top 5 m of the subsurface. Differences in packing and clay content control the measured velocities. Figure 4c shows velocities versus clay content for samples packed in the same way, for measurements made at about 0.1 MPa. Clay content is shown schematically below the plot in Figure 4c. We see in Figure 4c that although V_S decreases monotonically with increasing clay content, V_P initially increases as clay causes sand grains to stick together and fills dry pores. Then, V_P decreases with increasing clay content when the amount of clay is enough to form a continuous clay matrix through the sample. Similar behavior has been observed for sand-clay mixtures at 10 to 50 MPa (Marion et al., 1992). V_S does not show the same behavior. Apparently, the clay does not impede sliding between grains.

Table 1 shows velocity as a function of saturation for Ottawa sand samples. The water content was obtained from the water retention curve (Bonner et al., 2001). Velocity results and related uncertainties are described in detail elsewhere (Bonner et al., 1997, 1999a, 2000, 2001; Aracne-Ruddle et al., 1998, 1999; Berge et al., 1999). Our main findings are that the microstructure controls the velocities; the velocities are low, a few hundred m/s in dry samples, with V_P values being about twice the V_S values; velocities and amplitudes depend on the amount and distribution of fluid in saturated and drained samples; and the velocity gradients at the lowest pressures are strongly influenced by grain packing (Figure 4). Comparison of our laboratory velocity results to available seismic reflection and refraction data (e.g., Crouse et al., 1993; Taylor and Wilson, 1997; Bachrach et al., 1998; Boulanger et al., 1998; Steeples et al., 1999) showed agreement between velocities measured in

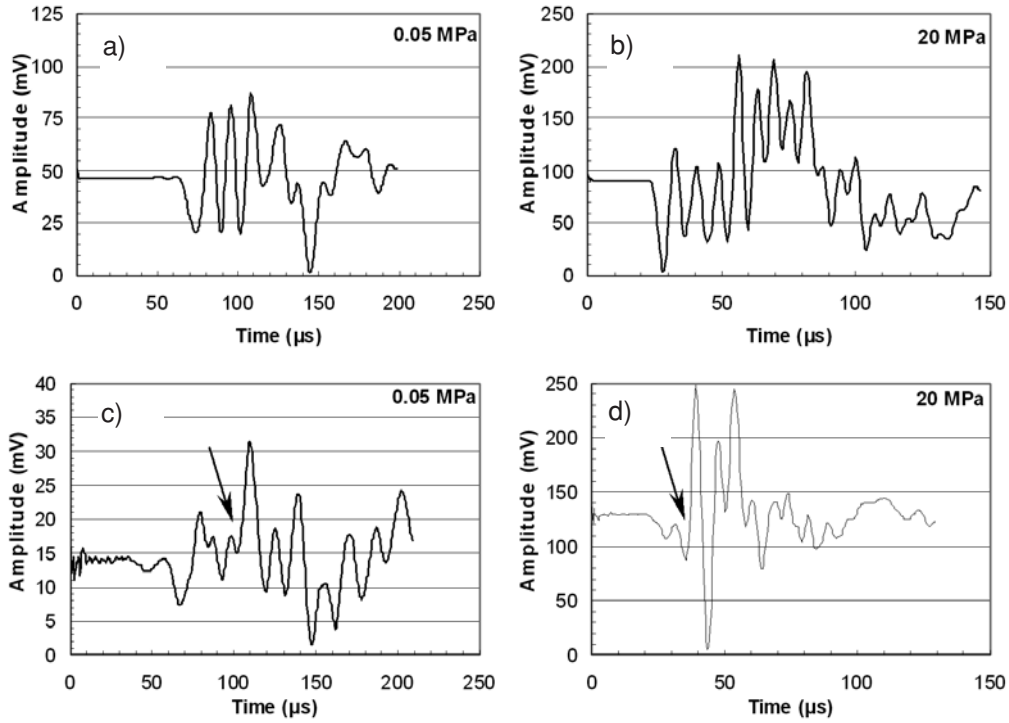

Figure 3. Typical signals from the Stanford experiment. P-wave signals in a sand sample are shown in (a) at 0.05 MPa and (b) at 20 MPa confining pressures. S-wave signals in a sand sample are shown in (c) at 0.05 MPa and (d) at 20 MPa confining pressures. Arrows in (c) and in (d) mark onset of the S-wave.

the lab and field for soils of similar types, at lab pressures equivalent to the appropriate depth for the field measurements (see also Table 2).

V_P and V_S results for sands from the Stanford experiments

Figure 5 shows the V_P and V_S results for four samples of the Santa Cruz aggregate tested in the Stanford hydrostatic apparatus. Details of our results are described in Zimmer et al. (2002a) and Zimmer et al. (2002b). The most important point relevant to shallow seismic applications is that the velocity-pressure dependence can be described for the S-waves by a fourth-root relation over the entire pressure range from 100 kPa to 20 MPa, while the P-wave dependence is closer to a fifth root dependence. The velocity data are very consistent between different samples and between different pressure cycles for the same sample. They also agree well with similar sand data from Domenico (1976), Prasad and Meissner (1992), Yin (1992), and Robertson et al. (1995). Velocity data from Prasad and Meissner (1992) are given in Table 3. Solid lines in Figure 5 represent empirical fits to the data.

Empirical fits to the velocity data in Figure 5 are of the form

$$V = a + bP^c, \tag{1}$$

where V is the velocity (m/s), and P is the pressure (MPa). These empirical fits demonstrate a velocity dependence to approximately the fifth root of the pressure. The exact empirical coefficients for each case are given in Table 4.

Attenuation results

As seismic waves pass through sediments and rocks, they lose energy. This attenuation or dissipation of seismic wave energy is greater in the loose sediments typical of the shallow subsurface. Since attenuation depends, among other factors, on material properties, it can potentially be used to predict these properties. Futterman (1962) defines the dissipation Q^{-1} (inverse of quality factor Q) as the ratio of energy loss per cycle (ΔE) to the maximum energy (E) stored in the system:

$$Q^{-1} = \frac{\Delta E}{2\Pi E} = (1 - \exp(\frac{4\Pi V_i}{V_r}))2\,\pi\,, \tag{2}$$

where the complex velocity $V = V_R + iV_i$.

O'Connell and Budiansky (1977) have shown that the quality factor can also be described in terms of the complex moduli as

$$Q = \frac{M_r}{M_i}, \tag{3}$$

where the complex modulus $M = M_R + iM_i$. Thus, Q_P, the P-wave quality factor is

$$Q_P = \frac{K_r + \frac{4}{3}\mu_r}{K_i + \frac{4}{3}\mu_i}, \tag{4}$$

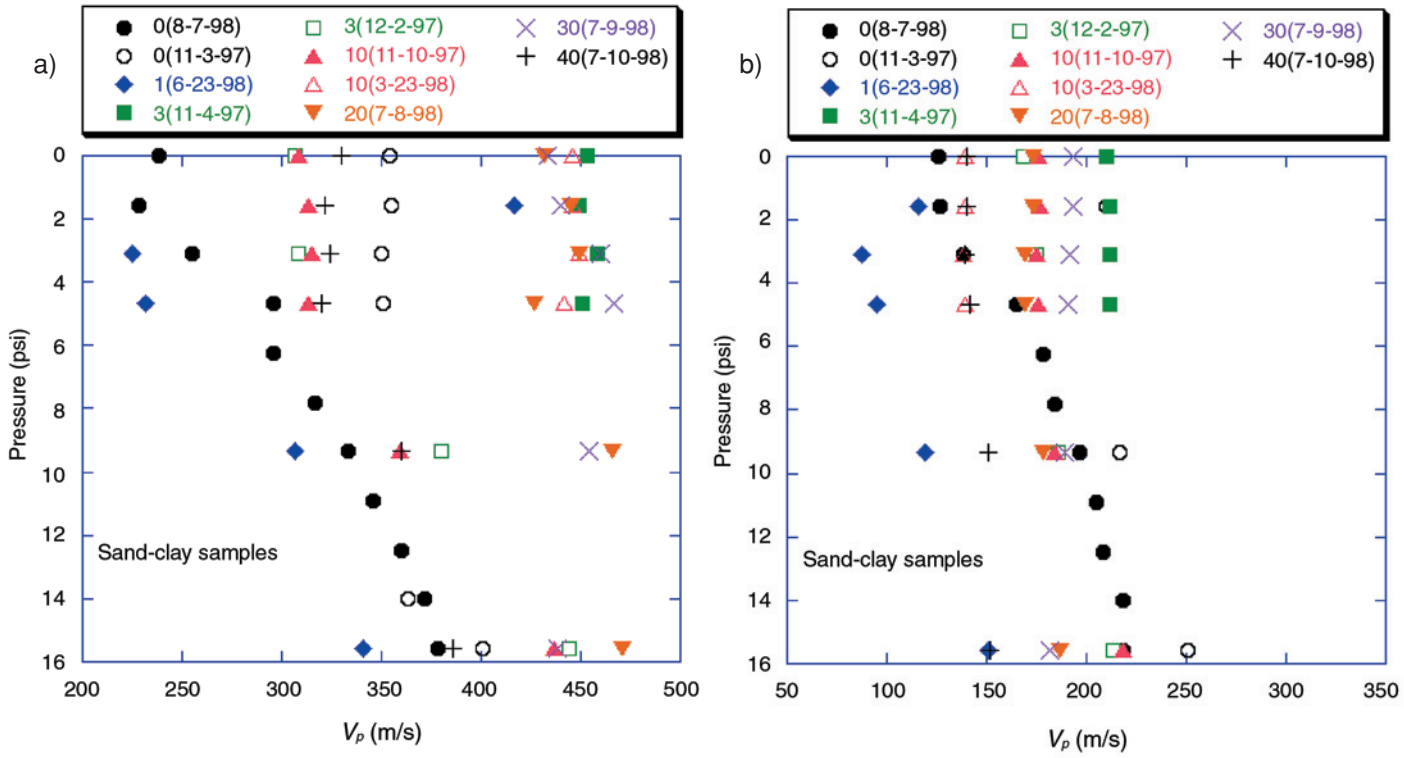

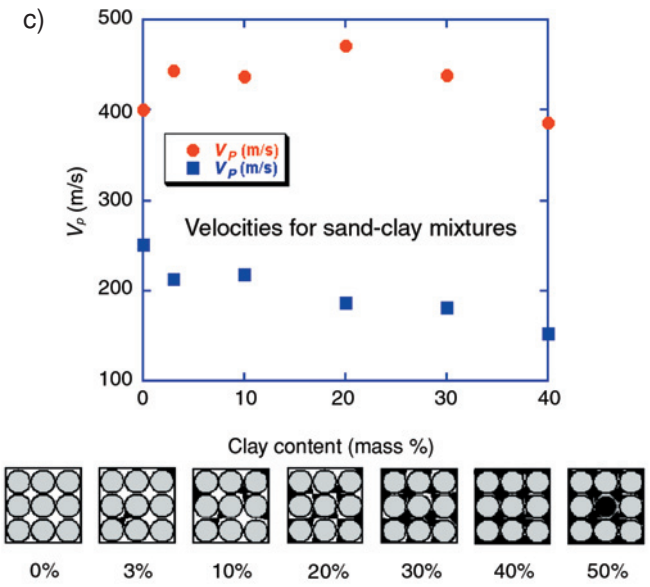

Figure 4. (a) V_P and (b) V_S versus pressure for various sand-clay mixtures. Numbers in legend of plot refer to date of measurement and clay content (by mass) for sand-clay mixtures. Different samples had different packing in some cases. (1 MPa = 145 psi). (c) (top) Velocity versus clay content for dry sand-clay mixtures at 16 psi (0.11 MPa) and (bottom) schematic diagram of microstructure for various amounts of clay (black) mixed with sand grains (gray circles).

Table 1. LLNL velocity results for partially-saturated sand samples at 40 kPa load

Waveform	V_P (m/s)	V_S (m/s)	Poisson's ratio	Notes
Sample 1:				
6/27/00 no. 1	375 ± 75	232 ± 6	0.19	Saturated, but some bubbles. (V_P = 1500 ± 40 through sat. patches)
Sample A:				
6/29/00 no. 2	357 ± 30	214 ± 10	0.22	Saturated, no visible bubbles
6/30/00 no. 1	308 ± 10	214 ± 10	0.03	Draining (capillary press = 35 cm), water content 22 to 28 %.
6/30/00 no. 3	326 ± 10	204 ± 6	0.18	Draining (capillary press = 44 cm), water content 13 to 17 %.
12/7/00	349 ± 8	249 ± 20	~0	Dried (chemical alteration probable)

Table 2. Poisson's ratios for dry samples at low pressures.

Clay content	Pressure	V_P/V_S	Poisson's ratio
0%	~0 MPa	1.7–2.2	0.23–0.36
0%	~0.1 MPa	1.6–2.1	0.18–0.36
1%	~0 MPa	3.6	0.46
1%	~0.1 MPa	2.3	0.38
3%	~0 MPa	1.8–2.2	0.29–0.36
3%	~0.1 MPa	2.1–2.2	0.35–0.37
10%	~0 MPa	1.8–3.2	0.26–0.45
10%	~0.1 MPa	2.0–3.2	0.33–0.45
20%	~0 MPa	2.5	0.4
20%	~0.1 MPa	2.5	0.41
30%	~0 MPa	2.2	0.38
30%	~0.1 MPa	2.4	0.4
40%	~0 MPa	2.4	0.39
40%	~0.1 MPa	2.5	0.41

and Q_S, the S-wave quality factor is

$$Q_S = \frac{\mu_r}{\mu_i}, \tag{5}$$

where K is the complex bulk modulus and μ is the complex shear modulus. Winkler and Nur (1982) have shown that a plot of Q_P/Q_S versus $(V_P/V_S)^2$ allows us to differentiate between the losses in bulk (K_i/K_r) and in shear (μ_i/μ_r). Prasad and Meissner (1992) and Prasad (2002) have shown that using both P- and S-wave velocity and attenuation allows us to differentiate between grain size and saturation in sands. Figure 6 shows a plot of $(V_P/V_S)^2$ versus Q_P/Q_S for dry and fully water-saturated sands. The figure shows that velocity and attenuation data can be useful tools to distinguish between different lithologies and between pres-

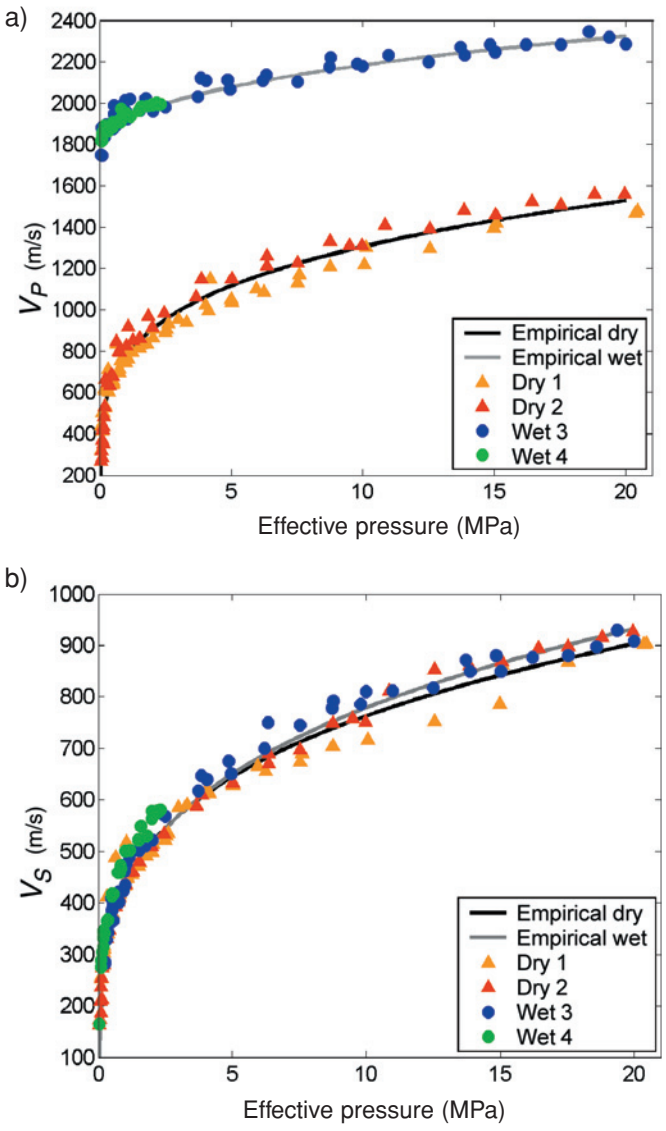

Figure 5. Ultrasonic velocity results for dry and water-saturated samples of the Santa Cruz aggregate. (a) V_P and (b) V_S for the four sand samples.

sure and saturation effects. Whereas, V_P is low at both low effective pressures and in gas saturated sands, V_S is unaffected by saturation state and is extremely low at low effective pressures. Thus, V_P/V_S ratio will move in different directions for the dry and the saturated cases. In addition to low V_P/V_S ratios, dry sands also have fairly high Q_P/Q_S values. Analyses of the main loss mechanism (Prasad and Meissner, 1992) (solid lines in Figure 6) show that the shear losses equal bulk losses in the dry sands; bulk losses are predominant in saturated sands. Increasing effective pressure decreases Q_P/Q_S and V_P/V_S ratios in both cases.

Discussion and Relevance to Shallow Seismic Measurements

Field seismic studies in the past decade have shown measurements of extremely low velocities for the shallow subsurface (e.g., Crouse et al., 1993; Taylor and Wilson, 1997; Bachrach et al., 1998; Carr et al., 1998; Steeples et al., 1999). Due to an absence of rock physics data corresponding to such sites, interpretation of sediment properties from seismic surveys has been limited to areas where ground-truth was provided by boreholes or existing geological descriptions. Added to this lack of data is the fact that most theoretical models of unconsolidated granular media fail to predict both P- and S-wave velocities realistically. Specifically, they do not predict the very low velocities and very steep gradients that are measured in the field. This breakdown of the theoretical models has lead to uncertainties in interpretations of field seismic measurements. Our laboratory measurements of ultrasonic velocities corroborate the low velocities and high gradients observed in the seismic surveys mentioned above. The agreement between laboratory and field measurements shows that theoretical models are, at best, an oversimplification of the natural case and modifications are required for accurate predictions of natural phenomena. A further consequence of the inadequacy of the velocity models arises when analyzing Poisson's ratio values. The theoretical smooth contact radius models predict Poisson's ratio values much lower than 0.1 (Winkler, 1983; Prasad and Meissner, 1992; Bachrach et al., 1998). By adding grain roughness, Palciauskas (1992) has shown that the Poisson's ratio can be as high as 0.14. Our measured Poisson's ratio in dry sands at very low pressures lies around 0.18–0.36 (Table 4). At these low pressures in the laboratory, Poisson's ratio does not depend significantly on pressure or on partial saturation. However, after addition of clay or at full saturation, Poisson's ratio values rise to about 0.4, close to fluid values (Table 3). At very low pressures, velocity is strongly dependent on composition, microstructure, and pressure.

Our results of velocities in sediments can be used for characterizing physical properties of sediments from field seismic surveys. They may also be useful for site-specific modeling. For example, Bertete-Aguirre and Berge (2002) have shown that having shear velocities available as well as P-velocities significantly improves the ability to recover lithology from seismic data even when the velocity uncertainties are high.

Table 3. Poisson's ratios for dry and saturated samples at hydrostatic pressures.

Pressure (MPa)	V_P (m/s)	V_S (m/s)	V_P/V_S	Poisson's ratio
		DRY		
0.0	275	160	1.72	0.24
0.101	501	235	2.13	0.36
0.15	500	268	1.87	0.30
0.201	510	290	1.76	0.26
0.3	549	330	1.66	0.22
0.5	640	365	1.75	0.26
1.02	821	434	1.89	0.31
2.46	982	534	1.84	0.29
5.03	1131	631	1.79	0.27
7.52	1225	697	1.76	0.26
9.97	1309	750	1.75	0.26
15.05	1445	861	1.68	0.22
17.54	1504	895	1.68	0.23
19.96	1566	925	1.69	0.23
		SATURATED		
0.111	1810	244	7.42	0.49
0.2	1836	271	6.77	0.49
0.292	1877	338	5.53	0.48
0.5	1883	378	4.87	0.48
1.049	1938	477	4.05	0.47
2.499	1973	569	3.48	0.45
4.947	2062	651	3.18	0.44
7.52	2108	752	2.83	0.43
9.792	2180	786	2.79	0.43
15.017	2246	850	2.65	0.42
17.526	2285	880	2.60	0.41
19.992	2286	908	2.52	0.41

Table 4. Empirical fits to the velocity data for Santa Cruz aggregate samples (between 0.1 and 20 MPa).

	a	b	c	1/c (root)	R^2
V_S — dry	0	436	0.243	4.11	0.9852
V_S — wet	0	428	0.260	3.84	0.9572
V_P — dry	0	774	0.227	4.40	0.9656
V_P — wet	1753	168	0.408	2.45	0.9295

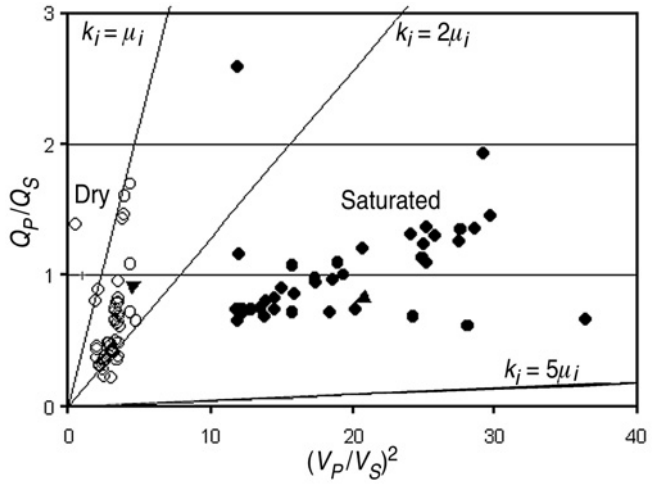

Figure 6. Separation of saturation effects using a loss diagram (Prasad and Meissner, 1992). Water-saturated sands (filled circles) are characterized by high V_P/V_S and Q_P/Q_S values, whereas dry sands (open triangles) have low V_P/V_S values but high Q_P/Q_S. The solid lines are calculations for various values of bulk (K_i) and shear (μ_i) losses. Shear losses are as high as bulk losses in dry sands, whereas in saturated sands, shear losses are higher. V_P/V_S and Q_P/Q_S values decrease with confining pressure as marked by arrows (data from Prasad and Meissner, 1992; and Prasad, 2002).

In a simplified, typical shallow sediment environment, the vadose zone consists of dry to partially saturated sediments. Below the water table, these sediments are water saturated (e.g., Hübner et al., 1985; Robertson et al., 1995; Bachrach et al., this volume). Depth of the water table will depend on the geographic location and on climatic conditions. We consider, as an example, a typical shallow soil scenario in a clean sand environment where the water table lies at a depth of 50 m. Dry and partially saturated sands lie above the water table and fully saturated sands below it. Using our experimental results, we can now reconstruct the velocity profile of such a sediment packet as shown in Figure 7. A steep velocity gradient will be characteristic of the uppermost layer, as shown in Figure 7. The water table will be marked by strong V_P/V_S contrast. Details of composition and fabric will affect the velocities. For example, addition of clay to the sands in the dry region will decrease velocity even further. From Figure 4, addition of moderate amounts of clay increases V_P due to cementation and pore-filling effects. With larger amounts of clay, once clay becomes load-bearing, the V_P decreases. V_S, on the other hand, decreases monotonically with addition of clay. Thus, the laboratory measurements can be powerful predictive tools to interpret field seismic data from the shallow subsurface and to construct synthetic seismograms.

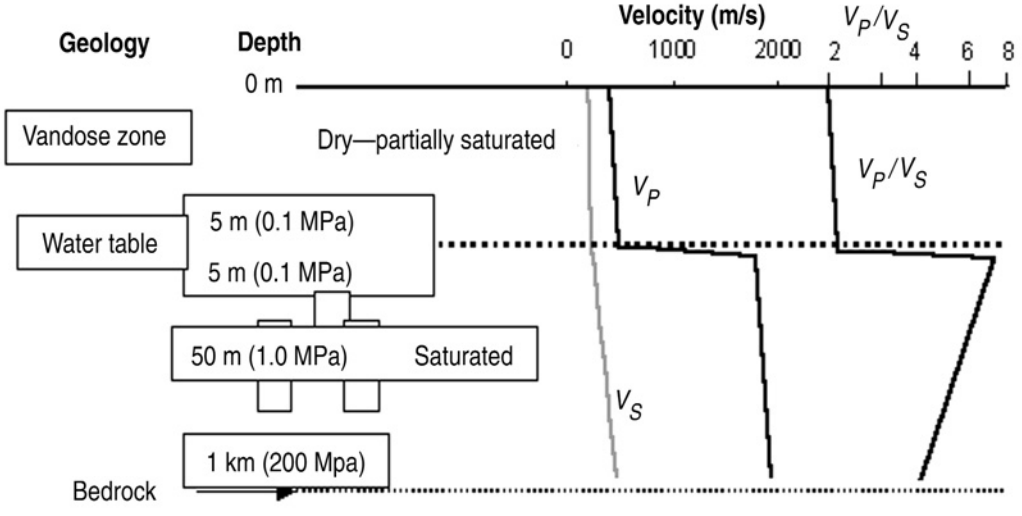

Figure 7. A typical shallow soil scenario in a clean sand environment and the V_P, V_S, V_P/V_S profile of such a sediment packet. The water table is clearly marked by high V_P/V_S ratios that decrease with depth. In the dry and the partially saturated zones, V_P/V_S values are low and they do not change much with pressure. In all cases, velocity is strongly dependent on depth.

Conclusions

We have shown the importance of conducting laboratory experiments at pressures relevant for the shallow depths typical for environmental geophysics. Our results on unconsolidated sediments show that in dry sands, the pressure dependence of P- and S-wave velocities can be empirically described by a fourth root (0.23–0.26). The P-velocity-dependence in wet sands lies around 0.4. At low pressures, velocity in dry sands shows a strong increase with pressure. Poisson's ratio values are low (0.18–0.3) at low pressures. Addition of water or clay to sands increases the Poisson's ratio to about 0.4.

Acknowledgments

Zimmer and Prasad's work was performed under the auspices of the Department of Energy (Award No. DE-FC26-01BC15354). Zimmer was also supported by a Chevron Stanford Graduate Fellowship. Work of Bonner and Berge was performed under the auspices of the U.S. Department of Energy by the University of California Lawrence Livermore National Laboratory under contract W-7405-ENG-48 and supported specifically by the Environmental Management Science Program of the Offices of Environmental Management and Science. Any opinions, findings, conclusions, or recommendations expressed herein are those of the authors and do not necessarily reflect the views of the DOE. We thank the reviewers for their comments.

References

Aracne-Ruddle, C., D. Wildenschild, B. Bonner, and P. Berge, 1998, Direct observation of morphology of sand-clay mixtures with implications for mechanical properties in sediments: Eos, Transactions of the American Geophysical Union, Fall Meeting Supplement, **79**, F820.

Aracne-Ruddle, C. M., et al., 1999, Ultrasonic velocities in unconsolidated sand/clay mixtures at low pressures: LLNL report UCRL-JC-135621, Lawrence Livermore National Laboratory. Available at http://www.llnl.gov/tid/lof/documents/pdf/237096.pdf; also summarized in Eos, Transactions of the American Geophysical Union, Fall Meeting Supplement, **80**, F397.

Bachrach, R., J. Dvorkin, and A. Nur, 1998, High-resolution shallow-seismic experiments in sand, Part II: Velocities in shallow unconsolidated sand: Geophysics, **63**, 1233–1284.

Bachrach, R., and T. Mukerji, 2005, Analysis of 3D high-resolution seismic reflection and crosswell radar tomography for aquifer characterization: A case study, this volume.

Baker, G. S., D. W. Steeples, and C. Schmeissner, 1999, In-situ, high-resolution P-Wave velocity measurements within 1 m of the earth's surface: Geophysics, **64**, 323–325.

Berge, P. A., et al., 1999, Comparing geophysical measurements to theoretical estimates for soil mixtures at low pressures, *in* M. H. Powers, L. Cramer, and R. S. Bell, eds., Proceedings of the 12th Annual Symposium on the Application of Geophysics to Engineering and Environmental Problems, 465–472.

Berge, P. A., and B. P. Bonner, 2002, Seismic velocities contain information about depth, lithology, fluid content, and microstructure: Expanded Abstracts of the Annual Symposium on the Application of Geophysics to Engineering and Environmental Problems, 12 PET.7, 1–15.

Bertete-Aguirre, H., and P. A. Berge, 2002, Recovering soil distributions from seismic data using laboratory velocity measurements: Journal of Environmental and Engineering Geophysics, **7**, 1–10.

Bonner, B. P., D. J. Hart, and P. A. Berge, 1997, Influence of chemistry on physical properties: Ultrasonic velocities in mixtures of sand and swelling clay (abstract): Eos, Transactions of the American Geophysical Union, Fall Meeting Supplement, **78**, F679.

Bonner, B. P., et al., 1999a, Ultrasonic characterization of synthetic soils for application to near-surface geophysics, *in* M. H. Powers, L. Cramer, and R. S. Bell, eds., Proceedings of the 12th Annual Symposium on the Application of Geophysics to Engineering and Environmental Problems, 455–463.

Bonner, B. P., P. A. Berge, and D. Wildenschild, 2001, Compressional and shear wave velocities for artificial granular media under simulated near surface conditions: 71st Annual International Meeting, SEG, Expanded Abstracts, 1419–1422

Bonner, B. P., C. Boro, and D. J. Hart, 1999b, Anti-waveguide for ultrasonic testing of granular media under elevated stress: LLNL Patent disclosure IL-10607, and patent application, DOE Patent Docket No. S-94-182.

Bonner, B. P., et al., 2000, Ultrasonic velocities of artificial sediments with minimal overburden: Eos, Transactions of the American Geophysical Union, Fall Meeting Supplement, **81**, F1105.

Boulanger, R. W., et al., 1998, Dynamic properties of Sherman Island peat: American Society of Civil Engineers, Journal of Geotechnical and Geoenvironmental Engineering, **124**, 12–20.

Carr, B. J., Z. Hajnal, and A. Prugger, 1998, Shear-wave studies in glacial till: Geophysics, **63**, 1273–1284.

Cheng, C. H., 1978, Seismic velocities in porous rocks: Direct and inverse problems: Ph.D. thesis, Masschusetts Institute of Technology.

Crouse, C. B., S. L. Kramer, R. Mitchell, and B. Hush-

mand, 1993, Dynamic tests of pipe pile in saturated peat: American Society of Civil Engineers Journal of Geotechnical Engineering, **119**, 1550–1567.

Domaschuk, L., and N. H. Wade, 1969, A study of bulk and shear moduli of a sand: Journal Soil Mechanics Foundation Division, Proc. American Society of Civil Engineers, **95**, 561–581.

Domenico, S. N., 1976, Effect of brine-gas mixture on velocity in an unconsolidated sand reservoir: Geophysics, **41**, 882–894.

Futterman, W. I., 1962, Dispersive body waves: Journal of Geophysical Research, **67**, 5279–5291.

Gassmann, F., 1951, Über die elastizität poröser medien: Vierteljahrsschrift der Naturforschenden Gesellschaft, **96**, 1–23.

Green, D. H., H. E. Wang, and B. P. Bonner, 1993, Shear wave attenuation in dry and saturated sandstone at seismic to ultrasonic frequencies: International Journal Rock Mechanics Mineral Science & Geomechanics Abstracts, **30**, 755–761.

Hamilton, E. L., and R. T. Bachman, 1982, Sound velocity and related properties of marine sediments: Journal of the Acoustical Society of America, **72**, 1891–1904.

Han, D., A. Nur, and F. D. Morgan, 1986, Effect of porosity and clay content on wave velocities of sandstones: Geophysics, **51**, 2093–2107.

Hübner, S., R. Meissner, and H. Stümpel, 1985, Einflüsse lithologischer Parameter oberflächennaher Sedimente auf Kompressions- und Scherwellengeschwindigkeiten, *in* Ingenieurgeologische Probleme in Grenzbereich zwischen Locker- und Festgesteinen, Springer-Verlag, 583–596.

Knight, R., and R. Nolen-Hoeksema, 1990, A laboratory study of the dependence of elastic wave velocities on pore scale fluid distribution: Geophysical Research Letters, **17**, 1529–1532.

Kuster, G. T., and M. N. Toksöz, 1974, Velocity and attenuation of seismic waves in two-phase media, Part I, Theoretical formulations, and Part II, Experimental results: Geophysics, **39**, 587–618.

Marion, D., A. Nur, H. Yin, and D. Han, 1992, Compressional velocity and porosity in sand-clay mixtures: Geophysics, **57**, 554–563.

OConnell, R. J., and B. Budiansky, 1977, Viscoelastic properties of fluid-saturated cracked solids: Journal of Geophysical Research, **82**, 5719–5735.

Palciauskas, V. V., 1992, Compressional to shear wave velocity ratios of granular rocks: Role of rough grain contacts: Geophysical Research Letters, **19**, 1683–1686.

Prasad, M., 2002, Acoustic measurements in sands at low effective pressure: Overpressure detection in sands: Geophysics, **67**, 405–412.

Prasad, M., and M. H. Manghnani, 1997, Effects of pore and differential pressures on compressional wave velocity and quality factor on Berea and Michigan sandstones: Geophysics, **62**, 1163–1176.

Prasad M., and R. Meissner, 1992, Attenuation mechanisms in sands: Laboratory versus theoretical (Biot) data: Geophysics, **57**, 710–719.

Rao, H. A. B., 1966, Wave velocities through partially saturated sand-clay mixtures: Response of Soils to Dynamic Loadings Report 24, Massachusetts Institute of Technology.

Robertson, P. K., S. Sasitharan, J. C. Cunning, and D. C. Sego, 1995, Shear-wave velocity to evaluate in-situ state of Ottawa Sand: Journal of Geotechnical Engineering, **121,** 262–273.

Santamarina, J. C., K. A. Klein, and M. A. Fam, 2001, Soils and waves: John Wiley and Sons.

Sears, F. M., and B. P. Bonner, 1981, Ultrasonic attenuation measurement by spectral ratios utilizing signal processing techniques: IEEE Transactions on Geoscience and Remote Sensing, **GE-19**, 95–99.

Steeples, D. W., G. S. Baker, C. Schmeissner, and B. K. Macy, 1999, Geophones on a board: Geophysics, **64**, 809–814.

Taylor, W. P., and C. D. V. Wilson, 1997, Tectonically influenced glacial erosion and ensuing valley infill: A geophysical survey: Quarterly Journal of Engineering Geology, **30**, 97–113.

Vernik, L., and A. Nur, 1992, Petrophysical classification of siliciclastics for lithology and porosity prediction from seismic velocities: Bulletin of the American Association of Petroleum Geologists, **76**, 1295–1309.

Wilkens, R. H., G. Simmons, T. M. Wissler, and L. Caruso, 1986, The physical properties of a set of sandstones—Part III. The effects of fine-grained pore-filling material on compressional wave velocity: International Journal of Rock Mechanics, Mineral Science and Geomechanical Abstracts, **23**, 313–326.

Winkler, K. W., 1983, Contact stiffness in granular porous materials. Comparison between theory and experiments: Geophysical Research Letters, **10**, 1073–1076.

Winkler, K. W., and A. Nur, 1982, Seismic attenuation: Effects of pore fluids and frictional sliding: Geophysics, **47**, 1–15.

Wyllie, M. R. J., A. R. Gregory, and L. W. Gardner, 1956, Elastic wave velocities in heterogeneous and porous media: Geophysics, **21**, 41–70.

Yin, H., 1992, Acoustic velocity and attenuation of rocks: Isotropy, intrinsic anisotropy, and stress induced anisotropy: Ph.D. thesis, Stanford University.

Zimmer, M. A., M. Prasad, and A. Nur, 2000, Ultrasonic velocities of sand at low effective pressures (abstract): Eos, Transactions of the American Geophysical Union, Fall Meeting Supplement, **81**, F1105–1106.

Zimmer, M. A., M. Prasad, and A. Nur, 2002a, Laboratory

P- and S-wave measurements on sands: Implications for pressure trends: Expanded Abstracts of the Annual Symposium on the Application of Geophysics to Engineering and Environmental Problems, 1–11 on CD.

Zimmer, M., M. Prasad, and G. Mavko, 2002b, Pressure and porosity influences on V_P-V_S ratio in unconsolidated sands: The Leading Edge, **21**, 178–183.